

Tomographic Dynamics and Scale-Dependent Viscosity in 2D Electron Systems

Patrick Ledwith¹, Haoyu Guo¹, Andrey Shytov², Leonid Levitov¹

¹Massachusetts Institute of Technology, Cambridge, Massachusetts 02139, USA

² School of Physics, University of Exeter, Stocker Road, Exeter EX4 4QL, United Kingdom

Fermi gases in two dimensions display a surprising collective behavior originating from the head-on carrier collisions. The head-on processes dominate angular relaxation at not-too-high temperatures $T \ll T_F$ owing to the interplay of Pauli blocking and momentum conservation. As a result, a large family of excitations emerges, associated with the odd-parity harmonics of momentum distribution and having exceptionally long lifetimes. This leads to “tomographic” dynamics: fast 1D spatial diffusion along the unchanging velocity direction accompanied by a slow angular dynamics that gradually randomizes velocity orientation. The tomographic regime features an unusual hierarchy of time scales and scale-dependent transport coefficients with nontrivial fractional scaling dimensions, leading to fractional-power current flow profiles and unusual conductance scaling vs. sample width.

Electron transport in many systems of current interest is governed by the processes of rapid momentum exchange in carrier collisions[1–4]. Disorder-free electron systems, in which the electron-electron (ee) collisions are predominantly momentum-conserving, can exhibit a hydrodynamic behavior reminiscent of that in viscous fluids [5–8]. Electron hydrodynamics, a theoretical concept describing this regime in terms of quasiparticle scattering near the Fermi surface, has been steadily gaining support in recent years [9–16].

It is usually taken for granted that hydrodynamics sets in at the lengthscales $r > l_{ee} = v/\gamma$ where $\gamma \sim T^2/T_F$ is the ee collision rate and v is Fermi velocity. Here we argue that in 2D systems—the focus of current experimental efforts[1–4]—our understanding of electron hydrodynamics requires a substantial revision. Indeed, generic large-angle quasiparticle scattering at a thermally broadened 2D Fermi surface is inhibited by fermion exclusion, except for the head-on scattering, which dominates angular relaxation (see Fig.1) [17–19]. The head-on collisions do lead to rapid momentum exchange between particles, however with one caveat. Such collisions change particle distribution in an identical way at momenta \mathbf{p} and $-\mathbf{p}$, providing relaxation pathway only for the part of momentum distribution which is *even* under Fermi surface inversion, $\delta f_{-\mathbf{p}} = \delta f_{\mathbf{p}}$. The odd-parity part $\delta f_{-\mathbf{p}} = -\delta f_{\mathbf{p}}$ does not relax due to such processes, giving rise to a large number of soft modes [20]. This peculiar behavior is generic in 2D at $T \ll T_F$, so long as the ee collisions are momentum-conserving.

The new regime, dominated by the head-on collisions and odd-parity harmonics, occurs at the lengthscales (and frequencies) in between the conventional ballistic and hydrodynamic regimes,

$$l_{ee} < r < \xi = \frac{v}{\sqrt{\gamma' \gamma}}, \quad (1)$$

where $\xi \gg l_{ee}$ is a new lengthscale originating from slowly relaxing odd-parity modes. Here the rate $\gamma \sim T^2/T_F$ describes head-on processes and even-parity modes, the rate $\gamma' \ll \gamma$ describes slow odd-parity modes. The intrinsic

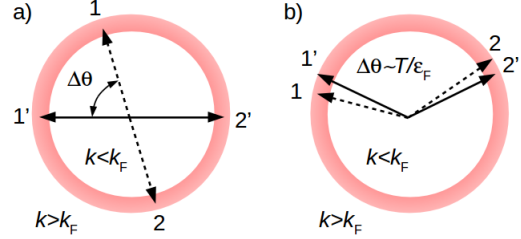


FIG. 1: Types of two-body collisions $1, 2 \rightarrow 1', 2'$ at a thermally broadened 2D Fermi surface (red rings), which are allowed by momentum and energy conservation and not inhibited by fermion exclusion. Head-on collisions (a) occur at a rate $\gamma \sim T^2/T_F$, with typical recoil $\Delta\theta \sim 1$. Such processes, however, affect only the even-parity part of momentum distribution. The odd-parity part, in contrast, relaxes solely due to small-angle scattering (b). Angular diffusion with a step $\Delta\theta \sim T/T_F \ll 1$ slows down the odd-parity relaxation, reducing the relaxation rate down to $\gamma' \sim T^4/T_F^3 \ll \gamma$.

γ' values due to small-angle ee scattering are estimated to be as low as [20]

$$\gamma' \sim (T/T_F)^2 \gamma \ll \gamma. \quad (2)$$

Since the rate γ' is small, in real systems it may be overwhelmed by extrinsic effects, such as phonons or disorder.

The conventional ballistic and hydrodynamic regimes occur at $r < l_{ee}$ and $r > \xi \gg l_{ee}$, respectively. In the ballistic regime the system features a standard free-particle behavior. Likewise, in the hydrodynamic regime transport coefficients assume their conventional values, e.g. the standard result $\nu = v^2/4\gamma$ for kinematic viscosity. However, at the intermediate scales (1) transport coefficients acquire a dependence on the wavenumber, becoming scale-dependent with nontrivial scaling dimensions.

At this point one may ask why the quasiparticle lifetimes, evaluated from the many-body Green’s functions as $\frac{1}{2\tau} = \text{Im} \Sigma(\varepsilon, p)$, behave as $T^{-2}/\ln \frac{T_F}{T}$ (or, $\varepsilon^{-2}/\ln \frac{\varepsilon_F}{\varepsilon}$ at zero temperature) without showing any indication of the slow modes[21–25]. This is so because the lifetimes evaluated by the selfenergy method are dominated by the fastest decay pathway, with the slow pathways due to

long-lived modes providing a subleading contribution to the decay rates. A different scheme is therefore required for treating the slow and fast modes on equal footing.

Here we consider a simple model in which different harmonics of particle momentum distribution $\delta f_{\mathbf{p}} = \sum_m \delta f_m e^{im\theta}$, with the angle θ parameterizing the Fermi surface, relax at different rates. We will assume that the even- m harmonics relax at a constant rate $\gamma \sim T^2/T_F$, whereas the odd- m rates behave as $\gamma' m^p$ with $\gamma' \ll \gamma$:

$$\gamma_{m \text{ even}} = \gamma(1 - \delta_{m,0}), \quad \gamma_{m \text{ odd}} = \gamma' m^p (1 - \delta_{m,\pm 1}). \quad (3)$$

Zero values for $\gamma_{m=0,\pm 1}$ reflect particle number and momentum conservation.

Below we consider several different p values which describe different regimes of interest. The intrinsic relaxation mechanism due to ee collisions predicts the odd-parity relaxation with $p = 4$ [20]. In addition, we consider the cases $p = 2$ and $p = 0$. This is done for illustration as well as having in mind that, in real systems, the very long lifetimes due to intrinsic effects can be overwhelmed by extrinsic effects. Relaxation due to residual disorder, phonons or scattering at boundaries is described by $p = 0$, whereas small-angle scattering due to smooth disorder potential, leading to conventional angular diffusion, is described by $p = 2$. In these cases, γ' is governed by other effects than the ee interactions. The intrinsic m^4 scaling of the odd- m rates corresponds to angular superdiffusion, with γ' , given by Eq.(2), taking on a role of the angular diffusion coefficient (see Eqs.(9),(10) below).

It might seem surprising that the modes with high m values could impact transport properties, since particle density and current—the two quantities usually probed in experiments—are described by $m = 0, \pm 1$ harmonics. Qualitatively, the significance of the high- m modes can be understood on very general grounds in terms of the Fluctuation-Dissipation Theorem which mandates strong fluctuations for slowly-relaxing degrees of freedom. Strong fluctuations, in turn, translate into enhanced scattering for other degrees of freedom, provided those are coupled to the slow degrees of freedom.

To understand how different slow modes are coupled, we consider transport equation, linearized near the \mathbf{p} -isotropic equilibrium state:

$$(\partial_t + \mathbf{v}\nabla - I_{ee})\delta f_{\mathbf{p}}(t, \mathbf{x}) = 0. \quad (4)$$

Couplings between different angular harmonics arise from the $\mathbf{v}\nabla$ term. To elucidate these couplings, we transform Eq.(4) to the δf_m basis, $\delta f_{\mathbf{p}} = \sum_m \delta f_m e^{im\theta}$. For plane-wave modes $\delta f_{\mathbf{p}}(t, \mathbf{x}) \sim e^{i\mathbf{k}\mathbf{x} - i\omega t}$, in the δf_m basis Eq.(4) takes the form of a 1D tight-binding model in which the eigenvalues of I_{ee} and $\frac{ikv}{2}$ represent the on-site potential and nearest-neighbor hopping amplitudes:

$$(\gamma_m - i\omega)\delta f_m = \frac{ikv}{2}\delta f_{m+1} + \frac{ikv}{2}\delta f_{m-1} \quad (5)$$

(without loss of generality we choose $\mathbf{k} \parallel x$). The hopping terms in Eq.(5) arise since $\cos\theta f(\theta)$ Fourier-transforms to $\frac{1}{2}f_{m+1} + \frac{1}{2}f_{m-1}$. For γ_m values vanishing on every other site, as in Eq.(3) in the limit $\gamma'/\gamma \rightarrow 0$, one can construct a non-decaying ($\omega = 0$) Bloch eigenstate described by δf_m vanishing on all the decaying sites with $\gamma_m \neq 0$ but nonzero and alternating in sign on the non-decaying sites where $\gamma_m = 0$, namely

$$\delta f_{m=2s+1} = (-1)^s, \quad \delta f_{m=2s} = 0. \quad (6)$$

Eq.(6) represents a *dark eigenstate* which is infinitely long-lived. Furthermore, the system hosts an entire band of long-lived near-dark states, with the lifetimes diverging in proximity of the dark state. Since these states have nonzero overlaps with the $m = \pm 1$ harmonics that govern electric current, slow decay translates—by the fluctuation-dissipation theorem—into an enhancement of current fluctuations and higher conductivity. The latter, in turn, means reduced dissipation and lower viscosity.

The essential physics here resembles the slow-mode relaxation mechanism by Mandelshtam and Leontovich, and Debye, with the $m > 2$ harmonics playing the role of bath variables (see, e.g., [26] and references therein). Since mode coupling in Eq.(5) is proportional to kv , the impact of soft modes with high m is stronger at larger k . This can be seen as an underlying reason for transport coefficients such as conductivity and viscosity becoming scale-dependent.

Turning to evaluating transport coefficients, we consider flows induced by an in-plane electric field varying as $\mathbf{E}(\mathbf{x}) = \mathbf{E}_k \cos \mathbf{k}\mathbf{x}$. Small deviations from equilibrium are described by a linearized kinetic equation

$$(\partial_t + \mathbf{v}\nabla_{\mathbf{x}} - I_{ee})\delta f_{\mathbf{p}}(t, \mathbf{x}) = -e\mathbf{E}(\mathbf{x})\nabla_{\mathbf{p}}f_{\mathbf{p}}^{(0)}, \quad (7)$$

where $f_{\mathbf{p}}^{(0)}$ is the equilibrium distribution. The perturbed distribution $\delta f_{\mathbf{p}}$ is nonzero near the Fermi surface. Below we will focus on the shear flows, described by $\mathbf{E}_k \perp \mathbf{k}$.

Since the even and odd parts of the distribution $\delta f_{\mathbf{p}}(t, \mathbf{x})$ relax at very different rates, we employ an adiabatic approximation in order to “integrate out” the even-parity part and derive a closed-form equation for the odd-parity part. We first note that the only term in Eq.(7) that alters parity, $\mathbf{v}\nabla_{\mathbf{x}}$, transforms functions of odd parity to those of even parity, and vice versa. We can therefore decompose the distribution into a sum of an odd and an even contribution, $\delta f_{\mathbf{p}} = \delta f_{\mathbf{p}}^+ + \delta f_{\mathbf{p}}^-$, and write a system of coupled equations for these quantities:

$$\begin{aligned} (\partial_t - I_+)\delta f_{\mathbf{p}}^+(t, \mathbf{x}) + \mathbf{v}\nabla_{\mathbf{x}}\delta f_{\mathbf{p}}^-(t, \mathbf{x}) &= 0, \\ (\partial_t - I_-)\delta f_{\mathbf{p}}^-(t, \mathbf{x}) + \mathbf{v}\nabla_{\mathbf{x}}\delta f_{\mathbf{p}}^+(t, \mathbf{x}) &= -e\mathbf{E}(\mathbf{x})\nabla_{\mathbf{p}}f_{\mathbf{p}}^{(0)} \end{aligned} \quad (8)$$

where I_{\pm} denote the even- m and odd- m parts of I_{ee} . Since $I_+ = -\gamma$, the first equation yields a relation $\delta f_{\mathbf{p}}^+(t, \mathbf{x}) = -\frac{1}{\gamma}\mathbf{v}\nabla_{\mathbf{x}}\delta f_{\mathbf{p}}^-(t, \mathbf{x})$, valid at low frequencies $\omega \ll \gamma$, i.e. at the lengthscales $r \gg l_{ee}$. Plugging it

in the second equation and interpreting I_- as the angle diffusion operator,

$$I_- = \sum_{m \text{ odd}} -\gamma_m |m\rangle \langle m| \approx -\gamma'(i\partial_\theta)^p \quad (9)$$

yields a closed-form relation for $\delta f_{\mathbf{p}}^-$ that will serve as a master equation for the new transport regime

$$[\partial_t - D(\hat{\mathbf{v}}\nabla_{\mathbf{x}})^2 + \gamma'(i\partial_\theta)^p] \delta f_{\mathbf{p}}^-(t, \mathbf{x}) = -e\mathbf{E}(\mathbf{x})\nabla_{\mathbf{p}} f_{\mathbf{p}}^{(0)}, \quad (10)$$

where we defined $D = v^2/\gamma$. Eq.(10) describes ‘‘tomographic dynamics’’: fast one-dimensional spatial diffusion along unchanging direction of velocity \mathbf{v} accompanied by a slow angle diffusion that gradually randomizes the orientation of \mathbf{v} .

In the above derivation we ignored the $m = 0$ zero mode of I_+ since in the shear flows created by transverse fields $\mathbf{E}_{\mathbf{k}} \perp \mathbf{k}$ particle density remains unperturbed. An extension of Eq.(10) accounting for this mode will be discussed elsewhere. Zero modes of I_- with $m = \pm 1$ can be accounted for by replacing in Eqs.(9),(10) $\partial_\theta^2 \rightarrow \partial_\theta^2 - 1$. However, this change only matters in the long-wavelength hydrodynamic regime, at $r \gtrsim \xi$, but would not affect the behavior in the tomographic regime, Eq.(1). We therefore suppress such terms for the time being.

A perturbed momentum distribution can be obtained by inverting transport operator in Eq.(10). Passing to Fourier representation $\delta f_{\mathbf{p}}(t, \mathbf{x}) = \delta f_{\mathbf{p}} e^{-i\omega t + i\mathbf{k}\mathbf{x}}$ we write a formal operator solution of Eq.(10) as

$$\delta f_{\mathbf{p}} = -\frac{1}{\hat{L} - i\omega} e\mathbf{E}\nabla_{\mathbf{p}} f_{\mathbf{p}}^{(0)}, \quad \hat{L} = D(\hat{\mathbf{v}}\mathbf{k})^2 + \gamma'(i\partial_\theta)^p. \quad (11)$$

Writing $\mathbf{E}\nabla_{\mathbf{p}} f_{\mathbf{p}}^{(0)} = \mathbf{E}\mathbf{v} \frac{\partial f_{\mathbf{p}}^{(0)}}{\partial \varepsilon}$ and noting that $-\frac{\partial f_{\mathbf{p}}^{(0)}}{\partial \varepsilon} = \beta f_{\mathbf{p}}^{(0)}(1 - f_{\mathbf{p}}^{(0)}) \approx \delta(\varepsilon - \mu)$, we see that the resulting perturbation indeed peaks at the Fermi level. Shear flows arise when $\mathbf{E}_{\mathbf{k}} = \int d^2x e^{-i\mathbf{k}\mathbf{x}} \mathbf{E}(\mathbf{x})$ is transverse to \mathbf{k} ; without loss of generality here we take $\mathbf{E}_{\mathbf{k}} \parallel \hat{\mathbf{y}}, \mathbf{k} \parallel \hat{\mathbf{x}}$.

The transport operator \hat{L} acts on the Fermi surface parameterized by the angle θ ; it is a sum of two noncommuting contributions, $(\hat{\mathbf{v}}\mathbf{k})^2 = k^2 \cos^2 \theta$ and $(i\partial_\theta)^p$. One is diagonal in the θ -representation, the other is diagonal in the δf_m representation. Diagonalizing \hat{L} , therefore, represents a nontrivial task. Assuming that the eigenfunctions and eigenvalues of \hat{L} , defined by $\hat{L}\psi_n(\theta) = \lambda_n \psi_n(\theta)$, are known, we can write the inverse as

$$\left\langle \theta \left| \frac{1}{\hat{L} - i\omega} \right| \theta' \right\rangle = \sum_n \frac{\bar{\psi}_n(\theta) \psi_n(\theta')}{\lambda_n - i\omega} \quad (12)$$

Using Eq.(12) we proceed to evaluate current $j_{y,\mathbf{k}} = ev\nu_0 \oint \frac{d\theta}{2\pi} \sin \theta \delta f(\theta)$, where ν_0 is the density of states at ε_F . Plugging the angle dependence $\mathbf{E}\mathbf{v} = E v \sin \theta$ gives

$$\mathbf{j}_{\mathbf{k}} = e^2 v^2 \nu_0 \mathbf{E}_{\mathbf{k}} \oint \frac{d\theta}{2\pi} \oint \frac{d\theta'}{2\pi} \sin \theta \left\langle \theta \left| \frac{1}{\hat{L} - i\omega} \right| \theta' \right\rangle \sin \theta'. \quad (13)$$

We can rewrite this relation as $\mathbf{j}_{\mathbf{k}} = \sigma(k, \omega) \mathbf{E}_{\mathbf{k}}$ by introducing a scale dependent conductivity

$$\sigma(k, \omega) = e^2 v^2 \nu_0 \sum_n \frac{|\langle \sin \theta | \psi_n(\theta) \rangle|^2}{\lambda_n - i\omega} \quad (14)$$

The matrix elements $\langle \sin \theta | \psi_n(\theta) \rangle$ quickly decrease with n , allowing to estimate the sum in Eq.(14) by retaining only the $n = 0$ term. The lowest eigenvalue can be found by the variational method as

$$\lambda_0 = \min \langle \psi | \hat{L} | \psi \rangle \sim \min \left(Dk^2 \delta\theta^2 + \frac{\gamma'}{\delta\theta^p} \right) \quad (15)$$

Here the trial state is normalized, $\langle \psi | \psi \rangle = 1$, and is localized within the region of width $\delta\theta$ near the minima of $\cos^2 \theta$, i.e. around $\theta = \pm\pi/2$. The estimate in Eq.(15) gives the width $\delta\theta \sim (\gamma'/Dk^2)^{\frac{1}{2+p}}$ and the value

$$\lambda_0 \sim Dk^2 \left(\frac{\gamma'}{Dk^2} \right)^{\frac{2}{2+p}} \quad (16)$$

Plugging these values in Eq.(14) and setting $\omega = 0$, gives a scale-dependent DC conductivity

$$\sigma(k) \sim \frac{e^2 v^2 \nu_0}{Dk^2} \left(\frac{Dk^2}{\gamma'} \right)^{\frac{1}{2+p}} \sim k^{-2 + \frac{2}{2+p}} \quad (17)$$

The variational estimate that leads to this answer is valid provided $\delta\theta \ll 1$, which translates into the condition $k > (\gamma'/D)^{1/2} = 1/\xi$ identical to the upper limit in Eq.(1) which marks the tomographic-hydrodynamic crossover.

Viscosity scale dependence can now be inferred by comparing Eq.(17) to the conductivity $\sigma(k) = \frac{n^2 e^2}{\eta k^2}$ obtained from the Stokes equation $-\eta \nabla^2 \mathbf{v} = n e \mathbf{E}$, giving

$$\eta(k) \sim k^{-\frac{2}{2+p}}, \quad (18)$$

Eq.(18) predicts viscosity growing vs. lengthscale, in agreement with the qualitative picture discussed above. The scaling exponents are $-1/3$, $-1/2$ and -1 for the three cases $p = 4, 2, 0$ discussed beneath Eq.(3).

These results are valid for wavenumbers in the range $l_{ee}^{-1} > k > \xi^{-1}$, see Eq.(1). Larger values $k > l_{ee}^{-1}$ correspond to ballistic free-particle transport; smaller values $k < \xi^{-1}$ correspond to hydrodynamic transport. At $k\xi \sim 1$ our k -dependent viscosity values $\nu(k)$ match the standard hydrodynamic value $\eta_{\text{hydro}} = nmv^2/4\gamma$. At shorter lengthscales, $k\xi > 1$, the viscosity is reduced compared to η_{hydro} by a factor $(k\xi)^{\frac{2}{2+p}}$. The reduction in η is maximal at $k \sim l_{ee}^{-1}$, where $\eta(k)/\eta_{\text{hydro}} \sim (\gamma'/\gamma)^{\frac{1}{2+p}}$. This scale dependence implies that, somewhat unexpectedly, the system behavior is more fluid-like at smaller distances and more gaseous at larger distances.

Next, we demonstrate that scale dependence of σ and η manifests itself in a characteristic current distribution across sample crosssection, which is distinct from

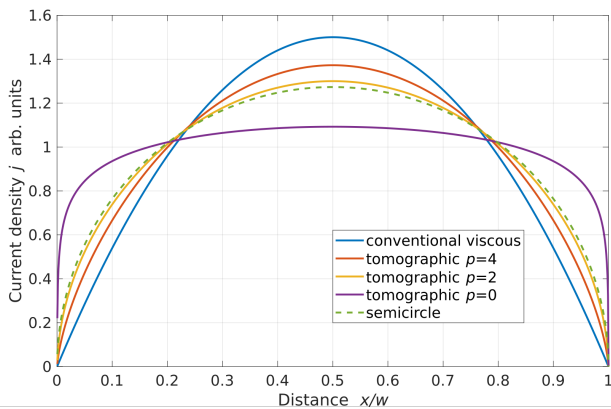


FIG. 2: Current density in a long strip of width w induced by a uniform DC electric field, Eq.(26). The flow profile is different for the viscous and tomographic regimes, showing signatures that depend on the angular relaxation dynamics type, parameterized by $p = 4, 2, 0$. A semicircle is shown as a guide to the eye.

the familiar parabolic distribution for conventional viscous flows. We analyze flow in a strip $0 < x < w$, $-\infty < y < \infty$ with momentum relaxation at the boundaries $x = 0, w$. To simplify the geometry, we consider an auxiliary problem in an infinite (x, y) plane equipped with an array of lines, spaced by w , where current relaxation may occur. Current induced by an E field, which is parallel to the lines, is given by

$$j(x) = \int dx' \sigma(x-x') [E - \alpha \sum_i j(x_i) \delta(x-x_i)], \quad (19)$$

with $x_i = wi$. Here α is a parameter that is a property of the lines, representing strip boundary, and $\sigma(x-x') = \int \frac{dk}{2\pi} e^{ik(x-x')} \sigma(k)$. The limit of interest to us is $\alpha \rightarrow \infty$.

Current distribution for this problem can be obtained by the Fourier method, by writing

$$j(x) = \sum_n j_n e^{k_n x}, \quad k_n = \frac{2\pi}{w} n, \quad n = 0, \pm 1, \pm 2, \dots \quad (20)$$

Plugging this expression in Eq.(19) and Fourier transforming, we have a system of coupled equations for j_n :

$$\rho_n j_n = E \delta_{n,0} - \tilde{\alpha} \sum_{n'} j_{n'}, \quad \rho_n = \frac{1}{\sigma(k_n)}, \quad (21)$$

where we defined $\tilde{\alpha} = \frac{\alpha}{w}$. These equations can be solved by separating the $n = 0$ and $n \neq 0$ harmonics,

$$(\rho_0 + \tilde{\alpha}) j_0 = E - \tilde{\alpha} \sum' j_{n'}, \quad j_n = \sigma(k_n) (-\tilde{\alpha} j_0 - \tilde{\alpha} \sum' j_{n'}). \quad (22)$$

where we introduced a shorthand notation $\sum' = \sum_{n' \neq 0}$. Taking a sum over all $n \neq 0$ harmonics yields a relation

$$(1 + \tilde{\alpha} G) \sum' j_n = -\tilde{\alpha} G j_0, \quad G = \sum' \sigma(k_n). \quad (23)$$

Expressing $\sum' j_{m'}$ and combining with the first equation in Eq.(22), we obtain

$$\left(\rho_0 + \frac{\tilde{\alpha}}{1 + \tilde{\alpha} G} \right) j_0 = E \quad (24)$$

For the case when there are no ohmic losses, $\rho_0 = 0$, and in the limit $\alpha \rightarrow \infty$, this relation simplifies to

$$j_0 = E \sum' \sigma(k_n). \quad (25)$$

The distribution of current within the strip then is

$$j(x) = j_0 \left(1 - \frac{\sum' \sigma(k_n) e^{ik_n x}}{\sum' \sigma(k_n)} \right). \quad (26)$$

For conventional scale-independent viscosity, plugging $\sigma(k) = \frac{1}{\nu k^2}$, this expression, after a little algebra, gives the familiar parabolic profile $j(x) \sim x(w-x)$. For scale-dependent viscosity $\nu(k) \sim k^{-\frac{2}{2+p}}$ it yields a distribution closely resembling the fractional-power profile

$$j(0 < x < w) \sim x^{\frac{2}{2+p}} (w-x)^{\frac{2}{2+p}}. \quad (27)$$

The resulting current profiles are illustrated in Fig.2 for several cases of interest. We see that the k dependence of σ and η has a strong impact on the current profile, providing a directly measurable signature of the tomographic regime.

This analysis points to several other interesting aspects of tomographic dynamics. First, the system conductance dependence vs. strip width can be obtained by noting that the sum in Eq.(25) converges rapidly, and is well approximated by the first term, $m = 1$. This predicts scaling for the conductance of the form

$$G(w) \sim w^{3-\frac{2}{2+p}}, \quad (28)$$

a dependence that *lies in between* the seminal Gurzhi scaling w^3 for the conventional viscous regime[5] and w^2 scaling for the ballistic transport regime[27].

Second, velocities of current-carrying electrons are tightly collimated along the strip axis, spanning angles in the range estimated above, $\delta\theta_{k_1} = (\xi k_1)^{-\frac{2}{2+p}} \ll 1$. This is in stark contrast to conventional viscous flows, where velocities are nearly isotropic. Strong velocity collimation tunable by the ee collision rate is a surprising behavior, which, along with the peculiar fractional-power conductance scaling, provides a clear signature of the tomographic regime.

Part of this work was performed at the Aspen Center for Physics, which is supported by National Science Foundation grant PHY-1607611. We acknowledge support by the MIT Center for Excitonics, the Energy Frontier Research Center funded by the US Department of Energy, Office of Science under Award de-sc0001088, and Army Research Office Grant W911NF-18-1-0116 (L.L.).

[1] M. J. M. de Jong, and L. W. Molenkamp, *Phys. Rev. B* **51**, 13389-13402 (1985).

- [2] D. A. Bandurin, I. Torre, R. Krishna Kumar, M. Ben Shalom, A. Tomadin, A. Principi, G. H. Auton, E. Kheshtanova, K. S. Novoselov, I. V. Grigorieva, L. A. Ponomarenko, A. K. Geim, and M. Polini, *Science* **351**, 1055-1058 (2016).
- [3] J. Crossno, J. K. Shi, K. Wang, X. Liu, A. Harzheim, A. Lucas, S. Sachdev, P. Kim, T. Taniguchi, K. Watanabe, T. A. Ohki, and K. C. Fong, *Science* **351** (6277), 1058-1061 (2016)
- [4] P. J. W. Moll, P. Kushwaha, N. Nandi, B. Schmidt, and A. P. Mackenzie, *Science* **351** (6277) 1061-1064 (2016)
- [5] R. N. Gurzhi, *Usp. Fiz. Nauk* **94**, 689 [Engl. transl.: *Sov. Phys. Usp.* **11**, 255 (1968)].
- [6] E. M. Lifshitz and L. P. Pitaevskii, *Physical Kinetics* (Pergamon Press 1981)
- [7] R. Jaggi, *J. Appl. Phys.* **69**, 816-820 (1991).
- [8] K. Damle and S. Sachdev, *Phys. Rev. B* **56**, 8714 (1997).
- [9] D. E. Sheehy and J. Schmalian, *Phys. Rev. Lett.* **99**, 226803 (2007).
- [10] L. Fritz, J. Schmalian, M. Müller, and S. Sachdev, *Phys. Rev. B*, **78** 085416 (2008).
- [11] M. Müller, J. Schmalian, and L. Fritz, *Phys. Rev. Lett.* **103** 025301 (2009).
- [12] A. V. Andreev, S. A. Kivelson, and B. Spivak, *Phys. Rev. Lett.* **106**, 256804 (2011).
- [13] D. Forcella, J. Zaanen, D. Valentinis, and D. van der Marel, *Phys. Rev. B* **90**, 035143 (2014).
- [14] A. Tomadin, G. Vignale, and M. Polini, *Phys. Rev. Lett.* **113**, 235901 (2014).
- [15] B. N. Narozhny, I. V. Gornyi, M. Titov, M. Schütt, and A. D. Mirlin, *Phys. Rev. B* **91**, 035414 (2015).
- [16] A. Principi, G. Vignale, M. Carrega, and M. Polini, *Phys. Rev. B* **93**, 125410 (2016).
- [17] B. Laikhtman, *Phys. Rev. B* **45**, 1259 (1992).
- [18] R. N. Gurzhi, A. N. Kalinenko, and A. I. Kopeliovich *Phys. Rev. Lett.* **74**, 3872 (1995)
- [19] H. Buhmann, L. W. Molenkamp, *Physica E* **12**, 715-718 (2002)
- [20] see Supplementary Online Material
- [21] A. V. Chaplik, *Zh. Eksp. Teor. Fiz.* **60**, 1845 (1971); [*Sov. Phys.—JETP* **33**, 997 (1971)].
- [22] C. Hodges, H. Smith, and J. W. Wilkins, *Phys. Rev. B* **4**, 302 (1971).
- [23] P. Bloom, *Phys. Rev. B* **12**, 125 (1975).
- [24] G. F. Giuliani and J. J. Quinn, *Phys. Rev. B* **26**, 4421 (1982).
- [25] A. V. Chubukov and D. L. Maslov, *Phys. Rev. B* **68**, 155113 (2003)
- [26] A. P. Levanyuk, *Sov. Phys. JETP* **22**, 901 (1966).
- [27] C. W. J. Beenakker, H. van Houten, *Sol. St. Phys.* **44**, 1 (1991).